Examination of the Community Multiscale Air Quality (CMAQ) model performance over the North American and European domains

K. Wyat Appel[a,*], Charles Chemel[b,c], Shawn J. Roselle[a], Xavier V. Francis[c], Ranjeet S. Sokhi[c], S.T. Rao[a] and Stefano Galmarini[d]

[a]Atmospheric Modeling and Analysis Division, National Exposure Research Laboratory, Office of Research and Development, United States
Environmental Protection Agency, RTP, NC, USA
[b]National Centre for Atmospheric Science, Centre for Atmospheric & Instrumentation Research, University of Hertfordshire, Hatfield, UK
[c]Centre for Atmospheric & Instrumentation Research, University of Hertfordshire, Hatfield, UK
[d]Joint Research Center, Institute for Environment and Sustainability, Ispra, Italy

*Corresponding author: Tel: +1 919 541 0757; fax: +1 919 541 1379. E-mail: appel.wyat@epa.gov. U.S. EPA-E243-04, Research Triangle Park, NC, 27711 USA

For submission to the Atmospheric Environment special issue on the AQMEII project

Abstract

The CMAQ modeling system has been used to simulate the air quality for North America and Europe for the entire year of 2006 as part of the Air Quality Model Evaluation International Initiative (AQMEII) and the operational model performance of O_3, fine particulate matter ($PM_{2.5}$) and PM_{10} for the two continents assessed. The model underestimates daytime (8am – 8pm LST) O_3 mixing ratios by 13% in the winter for North America, primarily due to an underestimation of daytime O_3 mixing ratios in the middle and lower troposphere from the lateral boundary conditions. The model overestimates winter daytime O_3 mixing ratios in Europe by an average of 8.4%. The model underestimates daytime O_3 by 4-5% in the spring for both continents, while in the summer daytime O_3 is overestimated (NMB = 9.8%) for North America but only slightly underestimated (NMB = -1.6%) for Europe. The model overestimates daytime O_3 in the fall for both continents, grossly overestimating daytime O_3 by over 30% for Europe. The performance for $PM_{2.5}$ varies both seasonally and geographically for the two continents. For North American, $PM_{2.5}$ is overestimated in the winter and fall, with an average NMB greater than -30%, while performance in the summer is relatively good, with an average NMB of -4.6%. For Europe, $PM_{2.5}$ is underestimated throughout the entire year, with the NMB ranging from -24% in the fall to -55% in the winter. PM_{10} is underestimated throughout the year for both North America and Europe, with remarkably similar performance for both continents. The domain average NMB for PM_{10} ranges between -45% and -65% for the two continents, with the largest underestimation occurring in the summer for North American and the winter for Europe.

Keywords: CMAQ; Ozone; Particulate Matter; Air Quality Modeling; Model Evaluation; AQMEII

1. Introduction

The Air Quality Model Evaluation International Initiative (AQMEII) is a model evaluation effort involving numerous research groups from North American and Europe with the goal of advancing the methods for evaluating regional-scale air quality modeling systems. As part of the AQMEII project, the Community Multiscale Air Quality (CMAQ; Foley et al., 2010) model has been applied to simulate air quality over North America (NA) and Europe (EU) for the year 2006.

The CMAQ simulation performed for NA for this project is unique compared to the CMAQ simulations performed in the past for several reasons. First, the simulation was performed over a single domain that covers the entire CONUS and a large portion of Canada using 12-km by 12-km horizontal grid spacing. In the past, two separate simulations covering the eastern and western U.S. have been used instead of single, continuous domain. Second, the simulation utilizes meteorology provided by the latest version of the Weather Research and Forecasting (WRF) model, whereas previous CMAQ annual simulations have typically utilized meteorology provided by the 5th Generation Mesoscale Model (MM5; Grell et al., 1994). Finally, the CMAQ simulation utilizes boundary conditions provided by the Global and regional Earth-system Monitoring using Satellite and in-situ data (GEMS) product.

The analysis presented here focuses primarily on ozone (O_3) and particulate matter ($PM_{2.5}$ and PM_{10}), as these are pollutants for which both the NA and EU have established criteria for acceptable limits (e.g. National Ambient Air Quality Standards) and instituted numerous control strategies to reduce precursor emissions. The analysis presented here is intended to provide a broad overview of the operational performance of the CMAQ model for these pollutants for NA and EU, and compare and contrast significant similarities or differences in model performance for the two continents.

2. Data

2.1 Model Inputs and Configuration

The CMAQ model requires gridded meteorological and emissions data to simulate the formation, transport and fate of numerous atmospheric pollutants, including O_3 and PM. Meteorological data for the NA and EU simulations were provided by the Weather Research and Forecast (WRF) model (Skamarock et al., 2008). For NA, the WRF domain covered the CONUS and portions of Canada and Mexico using 12-km by 12-km horizontal grid spacing and 34-vertical layers extending up to 50 hPa. The simulation utilized the Pleim-Xu land surface model (LSM), ACM2 planetary boundary layer (PBL) scheme, Morrison mixed phase (MP) scheme, Kain-Fritsch2 cumulus parameterization (CuP) scheme and the RRTMG long-wave radiation (LWR) scheme. Lateral boundary conditions (BCs) were provided by the North American Model (NAM), available from the National Centers for Environmental Prediction.

For the EU CMAQ simulation, the WRF model was also used, but with a slightly different configuration to that of the NA WRF simulation more appropriate for simulating the Europe continent. The EU WRF simulation was performed using 18-km by 18-km horizontal grid spacing with 52 vertical layers, 11 of which were below 1-km. The simulation utilized the

NOAH LSM, Morrison (MP) scheme, Grell and Devenyi CuP scheme, and RRTMG LWR scheme. Initial and lateral BCs were provided by the European Center for Medium-Range Weather Forecasts (ECMWF) model. Outputs from the WRF simulations for both continents were preprocessed for input into CMAQ using v3.6 of the Meteorology-Chemistry Interface Processor (MCIP; Otte et al., 2005). More specific details regarding the WRF simulations, including references for the various schemes used and an operational performance evaluation of the simulations can be found in Vautard et al. (this issue).

The NA CMAQ model simulation used the AQMEII standard NA emissions dataset, which is based on a 12-km national U.S. domain with speciation for the Carbon-Bond 05 (CB05) chemical mechanism (Yarwood et al., 2005). The emission inventory and ancillary files were based on the 2005 emission modeling platform. The fire emissions were based on 2006 daily fire estimates using the Hazard Mapping System Fire detections and Sonoma Technology SMARTFIRE system. Continuous Emission Monitoring System (CEMS) data from 2006 was used for the electric generating units sector. Plume rise was calculated within the CMAQ model (in-line). Temporal allocation was done monthly for each day of the week with all holidays ignored. Emissions were preprocessed for the CMAQ model using the Sparse Matrix Operator Kernel Emissions (SMOKE; Houyoux et al., 2000).

The AQMEII standard EU emissions data were used for the EU CMAQ simulation and are based on the TNO (http://www.tno.nl/) inventory for 2005, which consists of anthropogenic emission from ten Selected Nomenclature for Air Pollution (SNAP) sectors and international shipping. The ten SNAP sectors are energy transformation, small combustion sources, industrial combustion, industrial processes, extraction of fossil fuels, solvent and product use, road transport, non road transport, waste handling, and agriculture. Biogenic emissions of isoprene and terpene, calculated using the Model of Emissions of Gases and Aerosols from Nature (MEGAN; Guenther and Wiedinmyer, 2007; Sakulyanontvittaya et al., 2008), are included on the same resolution as the anthropogenic emissions. The fire emissions were bases on 2006 daily fire estimates from the MODIS fire radiative power product using the FMI Fire Assimilation System FAS-FRP (Sofiev et al., 2009). Plume rise was calculated offline with SMOKE. A more detailed description of the emission used for the two continents is available in Pouliot et al. (this issue).

The CMAQ model configurations were similar for NA and EU, with both simulations utilizing version 4.7.1 (Foley et al., 2010) of the model. The NA simulation used 34-vertical layers (matched to the WRF model vertical layers) and 12-km horizontal grid spacing covering the CONUS, southern Canada and northern Mexico, while the EU simulation used 34 vertical layers (52 WRF vertical layers collapsed to 34 CMAQ vertical layers in MCIP) and 18-km horizontal grid spacing covering most of EU. Other model options employed that were common to both simulations include the CB05 chemical mechanism with chlorine chemistry extensions (Yarwood et al., 2005), the AERO5 aerosol module (Carlton et al, 2010), the Asymmetric Cloud Model 2 (ACM2) PBL scheme (Pleim, 2007a,b).

Both the NA and EU simulations utilized the standard AQMEII BCs provided by the Global and regional Earth-system Monitoring using Satellite and in-situ data (GEMS) product (http://gems.ecmwf.int/about.jsp), which assimilates modeled data and observations (surface and satellite) to provide data for meteorology and atmospheric gases including greenhouse gases, global reactive gases and global aerosols. A more detailed description of the GEMS data as used as boundary conditions can be found in Schere et al. (this issue).

2.2 Air Quality Observations

For NA the observed data used to assess the CMAQ model estimates are obtained from several observational networks available across the U.S. that measure a combination of gas, aerosol, wet deposition and meteorological variables. The primary sources of ground level O_3, $PM_{2.5}$ and PM_{10} mass measurements for the U.S. is the USEPA's Air Quality System (AQS). The AQS network is geographically diverse and spans the entire U.S. and is an excellent source of quality assured air quality measurements. Measurements of O_3 are hourly, while measurements of PM can be either hourly or daily averages (available every 1, 3 or 6 days), depending on the particular site configuration. For observations of $PM_{2.5}$, measurements from the AQS, the Chemical Speciation Network (CSN) and the Interagency Monitoring of Protected Visual Environments (IMPROVE) network are used. In additional to total $PM_{2.5}$, the CSN and IMPROVE networks provide measurements of particulate $SO_4^{=}$, NO_3^{-}, NH_4^{+}, EC and OC, along with a large number of other trace elements. The AQS is used to provide PM_{10} measurement data. For Canada, the National Air Pollution Surveillance (NAPS) network provides measurements of O_3 and $PM_{2.5}$.

The air quality networks in EU used to provide data for the present analysis are the AirBase network (http://www.eea.europa.eu/themes/air/airbase), the Automatic Urban and Rural (AURN; http://uk-air.defra.gov.uk/interactive-map) network and the EMEP (http://www.emep.int/index_facts.html) network. Each of these networks provides hourly and daily average data for a number species, including O_3, $PM_{2.5}$ and PM_{10}. Assessment of the model performance was accomplished using the Atmospheric Model Evaluation Tool (AMET; Appel et al., 2010), which can perform a vast number of different analyses and produce many different plots useful for assessing model performance. AMET was originally designed for the U.S. based air quality networks, but has been extended to incorporate observations available from air quality networks in EU.

3. Results

3.1 Ozone

Ozone is an important criteria pollutant for both NA and EU. Ozone mixing ratios are the highest in the summer as the production of O_3 is a photo-chemically driven reaction and the reactions are more efficient under higher temperatures. In the U.S., O_3 mixing ratios generally peak in July and August (Fig. 1), when temperatures are the highest and the sun angle is high. The pattern of O_3 mixing ratios in EU is similar to that of NA, with a peak in O_3 mixing ratios in June and July (Fig. 2). The current daily thresholds for O_3 in the U.S. and EU are based on the maximum daily 8-hr average O_3 value and are currently set to 75 ppb for the U.S. and 120 μgm^{-3} (~60 ppb) for EU. Since the O_3 standards for each continent are based on the daily maximum 8-hr average O_3, the analysis here is limited to just the daytime hours, where daytime is defined as 8am to 8pm local standard time (LST), when O_3 mixing ratios are the highest.

For NA, operational model performance for O_3 was generally consistent with previous CMAQ simulations (Eder and Yu, 2006; Tesche et al., 2006; Appel et al., 2007), with several notable exceptions. Performance of maximum 8-hr average O_3 in the winter (January - March) underperformed previous CMAQ simulations (Appel et al., 2007), with the model demonstrating a large underestimation of daytime O_3 (-13.4% domain-wide average) for that period (Table 1). Fig. 1 illustrates the large underestimation of O_3 for NA in the winter, while Fig. 3a presents a spatial plot of Normalized Mean Bias (NMB) for AQS sites for winter. The underestimation of O_3 in the winter is largest in the Northeast and Great Lakes regions of the U.S. and for most of the Canadian sites, with smaller underestimations in the southern U.S. For EU, the CMAQ system overestimates daytime O_3 in southwestern half of the domain and underestimates daytime O_3 in the northeastern half of the domain, including the United Kingdom, in the winter (Fig. 4a). The largest overestimations occur in northern Italy, primarily in Po River Valley, where a large number of sites have NMBs greater than 100%. The largest underestimations occur in the Czech Republic and Poland, where some sites have NMBs exceeding -70%.

Investigation of the poor wintertime performance for O_3 in the NA CMAQ simulation suggests that the lateral BCs used in the AQMEII CMAQ simulation are largely responsible for the poor performance (Schere et al. this issue). In order to determine the impact of the later BCs on the winter O3 model estimates, the CMAQ simulation was repeated using BCs provided by the global model GEOS-Chem (Bey et al., 2001) instead of the AQMEII default BCs which used GEMS. The O_3 time-series for the NA and EU CMAQ simulations using lateral BCs provided by the GEOS-Chem model are presented in Figs. 1 and 2 along with the base AQMEII CMAQ simulation. The large wintertime underestimation of daytime O_3 that is clearly evident in CMAQ simulation for NA using the GEMS derived BCs is not present in the CMAQ simulation that utilized GEOS-Chem BCs. Similarly, the CMAQ estimated O_3 in the simulation for EU using GEOS-Chem BCs is much higher in the winter and spring than the simulation using GEMS BCs.

Further comparison of the vertical profiles of observed and CMAQ estimated O_3 (not shown) indicated that the mid to lower tropospheric O_3 mixing ratios in the GEMS BCs were significantly underestimated, while the same comparison to the CMAQ estimated O_3 from the simulation using GEOS-Chem BCs showed no significant underestimation of lower tropospheric O_3 (see also Schere et al., 2011 for additional discussion of the GEMS data). The lower O_3 mixing ratios in the troposphere in the GEMS BCs result in lower ground-level O_3 mixing ratios, particularly in the winter when O_3 provided from the lateral boundaries contributes a significant portion of the CMAQ estimated ground-level O_3. In the summer, O_3 mixing ratios in the lower troposphere in the GEMS BCs are much more similar in magnitude to the mixing ratios in the GEOS-Chem BCs, which results in better agreement with observations. Schere et al. (this issue) describe similar results for a comparison between the CMAQ simulations for EU using GEMS and GEOS-Chem BCs, and note that the performance degrades in the lower troposphere when using the GEMS BCs.

For the spring, the site specific NMBs typically range between ±10% for much of North America, with slightly larger NMBs in the Northeast, Canada and California, where daytime O_3 is underestimated at some sites by 20% or more (Fig. 3b). For EU, there continues to be a strong differentiation in performance in the spring between the southwest and northeast portions of the domain that was seen in the winter, with O_3 being relatively unbiased (NMB within ±10%) in the southwest (the exception being northern Italy where O_3 is overestimated/underestimated by 50% at several sites). The daytime O_3 for sites in Germany, Poland and the Czech Republic is frequently underestimated by 10-30% in the spring (Fig. 4b). Similar to the simulation for NA, a contributing factor to the underestimation of O_3 in the spring is the underestimation of O_3 in the GEMS lateral BCs (see Schere et at. in this issue).

For the summer, daytime O_3 is overestimated over the majority of NA (domain average NMB = 9.8%), with the largest overestimations in California, Florida and along the Gulf of Mexico (Fig. 3c). The NMB for the Canadian NAPS sites in summer tends to be lower than that of the AQS sites. For EU, the daytime O_3 performance is generally better than that of NA, with a large number of sites having NMBs within ±10% and the majority of sites having NMBs with ±20% (Fig. 4c). The largest biases occur in France and northern Italy (Po River Valley), where O_3 tends to be underestimated by 10-20% for the majority of the sites, and along the coast of Spain, where the model typically overestimates daytime O_3 by 20% or more (slightly smaller overestimations occur along the coast of Italy as well). The overestimation of O_3 in the summer along coastal areas is seen in the CMAQ simulation for NA as well (Fig. 3c), suggesting that the source of the large biases may be due to errors in the meteorological inputs to the CMAQ system, particularly in regards to the meteorological model's ability to accurately represent the sea-breeze and land-breeze effects along the coast. The CMAQ model performance for the summer is consistent with a previous study by Eder et al. (2009) that reported CMAQ overestimated O_3 during the summer by about 9% and also noted very large overestimations along the Gulf of Mexico.

Daytime O_3 is overestimated in the fall for both NA and EU (Figs. 3d and 4d). The largest overestimations in NA occur in the eastern U.S. (including the eastern NAPS sites), where the NMB frequently exceed 20% at a large number of sites, and in the Northwest, where the NMB exceeds 80% at several of the NAPS sites. The fall has the worst overall performance for daytime O_3 for EU, with the model grossly overestimating O_3 across most of the domain (domain average NMB = 32.3%). The majority of sites have NMBs greater than 20%, with a large number of sites in northern Italy having NMBs exceeding 100%.

3.2 $PM_{2.5}$

Particulate matter, including both $PM_{2.5}$ with a diameter less than 2.5 µm and coarse PM_{10} with a diameter less than 10 µm, is an important air pollutant for which standards exist for both the U.S. and EU. The U.S. limits on PM are based on $PM_{2.5}$, with the current annual limit set at 15 μgm^{-3}, while for EU the primary PM standard is based on PM_{10}, with the current annual limit set at 40 μgm^{-3}. Since the two continents use different standards for regulating PM, the monitoring networks are also different, with North American (U.S. and Canada) networks focused primarily on measuring $PM_{2.5}$ and European networks focused on measuring PM_{10}. As such, PM_{10} measurements for NA are not as widely available as $PM_{2.5}$ measurements, and likewise there are limited $PM_{2.5}$ measurements available for EU. On average, there are approximately 870 AQS sites in the U.S. and 160 AirBase sites in EU with $PM_{2.5}$ measurements, and 580 AQS sites and over 1000 AirBase sites with PM_{10} measurements.

Unlike O_3, which has a large seasonal dependency, $PM_{2.5}$ concentrations in NA do not vary as much throughout the year (Fig. 5), while for EU high concentrations of $PM_{2.5}$ are observed from January through March, after which the concentrations are considerably lower and relatively constant throughout the remainder of the year (Fig. 6). The CMAQ model generally does well representing the small seasonal trends in $PM_{2.5}$ for both continents, and captures the synoptic forcing features. Note that there are a limited number of $PM_{2.5}$ observations available for EU, with the majority of the observations sites in Portugal, Spain, France, Italy, Belgium, Germany, and the Czech Republic.

For the winter, there is a large overestimation of $PM_{2.5}$ in NA (Table 2), with a domain-wide average NMB of 30.4% and Mean Bias (MB) of 3.4 μgm^{-3}, but underestimates $PM_{2.5}$ to an even greater extent in EU, with a NMB of -55% (MB = -12.9 μgm^{-3}). The largest underestimations in the NA occur in the west, where a large number of sites report NMBs greater than 100% (Fig. 7a). The northeastern U.S. also has a number of sites with NMBs exceeding 30%. For EU, the underestimation in $PM_{2.5}$ is systematic across the domain, with only a handful of sites reporting an overestimation (Fig. 8a). The largest underestimations occur in the Czech Republic, Germany and Italy, with the majority of sites reporting NMBs greater than -60%. The performance for France, the United Kingdom, Spain and Portugal is better, with a number of sites reporting NMBs smaller than -30%.

The overestimation in $PM_{2.5}$ in NA is primarily due to an overestimation of the unspeciated $PM_{2.5}$ mass, along with a smaller overestimation of elemental and organic carbon (Appel et al, 2008). The unspeciated $PM_{2.5}$ mass, sometimes referred to as PM_{other}, is comprised primarily of the non-carbon atoms associated with OC, along with trace elements (e.g. Fe, Mg, Mn, etc.), primary ammonium and other unidentified mass in the speciation profiles. Since this unspeciated mass makes up a significant portion of the total $PM_{2.5}$ mass and is often largely under or overestimated in the CMAQ model, efforts were made to include speciation of the unidentified mass, in particular the trace elements, in the model. The next version of the CMAQ model, due to be released in the fall of 2011, will include the speciation of the trace metals, allowing for a comparison of the model estimates to observations, which will hopefully lead to an improvement in the model estimates for those elements and reduction in the bias for PM_{other}.

The model estimates for $PM_{2.5}$ improve significantly in the spring, with a domain-wide average NMB of 18.9% (MB = 2.0 μgm^{-3}) for NA and -36.9% (MB = -5.8 μgm^{-3}) for EU (Table 2). For NA, $PM_{2.5}$ tends to be underestimated in the southern portion of the domain, with most sites having a NMB less than -20%, while $PM_{2.5}$ continues to be overestimated by the model in the Northeast and in the west, where most sites have a NMB of 20% or greater (Fig. 7b). For EU, $PM_{2.5}$ continues to be significantly underestimated in the east (Czech Republic and Italy), with the underestimation in Germany, France and the United Kingdom improved from the winter (Fig. 8b). The performance in Spain and Portugal is relative good, with most sites having a NMB within ±20%.

For the summer, CMAQ estimated $PM_{2.5}$ concentrations are slightly underestimated on average, with a domain-wide average NMB of -4.6% and MB of -0.6 μgm^{-3} (Table 2). Spatially, $PM_{2.5}$ is underestimated by 20-30% for majority of sites in the eastern U.S., the exceptions being Florida, where $PM_{2.5}$ is overestimated, and the Great Lakes region, where most sites have NMBs within ±10% (Fig. 7c). The underestimations in the southeastern U.S. may be due in part to an underestimation of secondary organic aerosol, which can make up a large portion of the total $PM_{2.5}$ in the southeast (Carlton et al., 2010). Large underestimations of $PM_{2.5}$ in the desert southwest (New Mexico, Arizona, Colorado and Utah) of -50% or more may be due to a lack of wind-blown dust in the model. The next version of the CMAQ model will include a method for representing wind-blown dust, which may improve the underestimations of $PM_{2.5}$ in the southwestern U.S. in the summer. For EU, the performance for the summer is similar to the spring, with a domain-wide average NMB of -37.2% (MB = -4.9 μgm^{-3}), and a similar spatial distribution of bias as the spring (Fig. 8c).

For the fall, $PM_{2.5}$ is again overestimated for NA, with a domain-wide average NMB of 36.3% (MB = 4.0 μgm^{-3}). The spatial pattern of bias is similar to that of the winter, with the largest overestimations in the northeast and northwest U.S. (Fig. 7d). As with the winter, the overestimation of the unspeciated $PM_{2.5}$ mass is largely responsible for the overestimation of $PM_{2.5}$ in the fall, along with smaller overestimations of particle nitrate and ammonium. For EU, $PM_{2.5}$ continues to be underestimated, however the bias is smaller than any of the other seasons, with an average NMB of -24.2% (MB = -3.8 μgm^{-3}). The largest underestimations continue to be in the Czech Republic and Italy, with most sites having NMBs of – 20% to -50% (Fig. 8d). Performance for sites in Germany, France the United Kingdom improves again, with most sites having NMBs within ±20%, while in Spain and Portugal several of the sites now show an overestimation of $PM_{2.5}$, generally within 30-50%.

3.3 PM_{10}

The PM_{10} mass is composed of all the PM less than 10 µm in diameter, and therefore includes all the $PM_{2.5}$ mass and coarse PM (PM_{10}- $PM_{2.5}$). Fig. 9 presents the domain-average time series for observed and CMAQ estimated PM_{10} for NA, while Fig. 10 presents a similar time-series plot for EU. The model systematically underestimates PM_{10} for both continents throughout the year, with the largest underestimation occurring in the winter for EU when observed PM_{10} is very high. For EU in the winter, the domain average NMB is -64.8% (MB = -21.5 µgm^{-3}), compared to only -47.6% (MB = -11.5 µgm^{-3}) for NA. For the other seasons, the underestimation for both continents is nearly identical and relatively consistent through the year, with the model underestimating PM_{10} by between 45-60% (11-16 µgm^{-3}) for each continent (Table 3).

Spatially, the model tends to demonstrate a similar bias pattern throughout the year for both continents. In the winter, when the PM_{10} underestimation is the smallest for NA, the model generally overestimates PM_{10} by 20-50% along the east coast of the U.S. (Fig. 11a). For the rest of country, PM_{10} is largely underestimated, particularly in the western U.S. (with the exception of areas right along the coast). For EU, almost every site shows an underestimation of PM_{10}, with most sites having NMBs exceeding -50% (Fig. 12a). The smallest biases are in northern

France, where most sites have NMBs less than 30%. In the spring, the bias pattern is similar to the winter, with the smallest biases for NA occurring along the east and west coasts, while in EU the bias spatial pattern is nearly identical to that of winter (Figs. 11b and 12b).

For the summer, the majority of sites in NA now show some level of underestimation of PM_{10}, with almost all the sites in the western U.S. having NMBs greater than -20% (Fig. 11c). For EU, the bias pattern is again similar to the winter and spring, with only northern France and Portugal having any significant number of sites showing NMBs smaller than 40% (Fig. 12c). The bias tends to improve in the fall for both continents compared to the summer, with a large number of sites in the eastern U.S. having NMBs between ±30%, while in the western U.S. most sites continue to show large underestimations of PM_{10} of 50% or more (Fig. 11d). For EU, the majority of sites continue to show significant underestimations of PM_{10} in the fall (Fig. 12d), however a large number of sites in France and Germany now have NMBs between -20 to -30%, an improvement of the -40% or more NMBs seen in the other seasons. Additional analysis is needed to diagnose the cause for the large biases in CMAQ PM_{10} estimates, which are likely due to a combination of errors in the emissions inventory and chemical transport model.

4. Summary

The CMAQ modeling system has been used to simulate NA and EU for the entire year of 2006. The model performance for O_3 varies seasonally, with the model underestimating daytime O_3 mixing ratios in the winter by about 13% for NA and overestimating daytime O_3 for EU by roughly 8%. Analysis suggests that lower O_3 mixing ratios in the middle and lower troposphere from the chemical boundary conditions are primarily responsible for the lower ground-level O_3

mixing ratios in the winter in NA and EU. For the spring, daytime O_3 is slightly underestimated for both NA and EU (4-5%), likely due in part to an underestimation of O_3 from the boundaries. For the summer, when O_3 mixing ratios are the highest, CMAQ overestimates daytime O_3 for NA by about 10% on average, while for EU the model underestimates daytime O_3 by less than 2% on average. Daytime O_3 continues to be overestimated in the fall for NA by 8% on average, while for the EU the model grossly overestimates O_3 by more than 30% on average. Overall, the model demonstrates relatively similar performance for daytime O_3 in both modeling domains, with the exception of the fall.

The model performance for $PM_{2.5}$ varies between the two continents, with the model overestimating $PM_{2.5}$ in the winter, spring and fall, and being relatively unbiased in the summer for NA, while for EU the model underestimates $PM_{2.5}$ throughout the entire year. While it is not clear what is driving the bias in $PM_{2.5}$ for the two continents, likely sources of error for both continents is the lateral boundary conditions and emissions. It would be helpful to examine any speciated $PM_{2.5}$ data available in EU to determine what components of $PM_{2.5}$ are primarily responsible for the underestimation. The model performance for PM_{10} was also examined for both continents, with the model systematically underestimating PM_{10} for both continents. Outside of the winter months, when PM_{10} was grossly underestimated for EU, the model performance for PM_{10} for both continents is very similar, with model generally underestimating PM_{10} between 45-60% on average. More investigation is needed to determine what is driving the poor PM_{10} estimates from the modeling system (e.g. emissions or meteorology). Segregating the data by different synoptic regimes (e.g. Appel et al., 2007) may highlight the role meteorology plays in the PM_{10} estimates, while the addition of trace metals and a method for tracking wind-blown dust available in the next release of the CMAQ model may help illuminate errors in the emission inventory.

The analysis presented here represents only a broad overview of the operational model performance of three pollutants for NA and EU. The analysis describes some the similarities and differences in model performance between the two continents and highlights aspects of the modeling system that need improvement (e.g. PM_{10}). Further analysis is needed to determine the factors driving these differences in model performance. Future work will include comparing the model performance for other species, such as NO_2 and SO_2, between the two continents, as well as examining the performance of the model wet deposition estimates, which are important outputs used in ecological studies.

Acknowledgements

We gratefully acknowledge the contributions of various groups to the first Air Quality Model Evaluation International Initiative (AQMEII) activity. The following agencies have prepared the datasets used in the preparation phase of this study: U.S. EPA (North American emissions processing and gridded meteorology); U.S. EPA, Environment Canada, Mexican Secretariat of the Environment and Natural Resources (Secretaría de Medio Ambiente y Recursos Naturales-SEMARNAT), and National Institute of Ecology (Instituto Nacional de Ecología-INE) (North American national emissions inventories); TNO (European emissions processing); Laboratoire des Sciences du Climat et de l'Environnement, IPSL, CEA/CNRS/UVSQ (gridded meteorology for Europe); and ECMWF/GEMS project and Météo-France/CNRM-GAME (Chemical boundary conditions). Ambient North American concentration measurements were extracted from Environment Canada's National Atmospheric Chemistry Database (NAtChem) PM database and provided by several U.S. and Canadian agencies (AQS, CAPMoN, CASTNet, IMPROVE, NAPS, SEARCH, and STN networks); North American precipitation-chemistry measurements were extracted from NAtChem's precipitation-chemistry database and were provided by several U.S. and Canadian agencies (CAPMoN, NADP, NBPMN, NSPSN, and REPQ networks); the WMO World Ozone and Ultraviolet Data Centre (WOUDC) and its data-contributing agencies provided North American and European ozonesonde profiles; NASA's Aerosol Robotic Network (AeroNet) and its data-contributing agencies provided North American and European AOD measurements; the MOZAIC Data Centre and its contributing airlines provided North American and European aircraft takeoff and landing vertical profiles. For European air-quality data, the EMEP European Environment Agency/European Topic Center on Air and Climate Change/AirBase provided European air- and precipitation chemistry data. Data from meteorological station monitoring networks were provided by NOAA and Environment Canada (for the U.S. and Canadian meteorological network data) and the National Center for Atmospheric Research (NCAR) data support section. Joint Research Center Ispra/Institute for Environment and Sustainability provided its ENSEMBLE system for model-output harmonization and analyses and evaluation.

The authors would like to extend a special note of thanks to the Computer Sciences Corporation for performing the WRF simulation, emissions processing and CMAQ model simulations for North America. This work was partially supported by the University of Hertfordshire under the TEMPO project awarded through its Small Research Grants Competition. We would like to thank Guido Pirovano (INERIS, France and RSE, Milan, Italy) for his help in setting up AMET for Europe.

The views expressed here are those of the authors and do not necessarily reflect the views and policies of the U.S. Environmental Protection Agency or any other organization participating in the AQMEII project. This manuscript has been subjected to U.S. EPA review and approved for publication.

References

Appel, K.W., Bhave, P.V., Gilliland, A.B., Sarwar, G., Roselle, S.J., 2008. Evaluation of the Community Multiscale Air Quality (CMAQ) model version 4.5: Sensitivities impacting model performance; Part II - particulate matter, Atmospheric Environment 42, 6057-6066.

Appel, K.W., Gilliand, A.B., Sarwar, G., Gilliam, R.C., 2007. Evaluation of the Community Multiscale Air Quality (CMAQ) model version 4.5: Sensitivities impacting model performance; Part I – ozone, Atmospheric Environment 41, 9603-9615.

Appel, K. W., Gilliam, R. C., Davis, N., Zubrow, A., and Howard, S. C., 2010. Overview of the Atmospheric Model Evaluation Tool (AMET) v1.1 for evaluating meteorological and air quality models, Environmental Modeling and Software, doi:10.1016/j.envsoft.2010.09.007.

Bey, I., Jacob, D.J., Yantosca, R.M., Logan, J.A., Field, B.D., Fiore, A.M., Li, Q., Liu, H.Y., Mickley, L.J., and Schultz, M.G., 2001. Global modeling of tropospheric chemistry with assimilated meteorology: Model description and evaluation, Journal of Geophysical Research, 106, 23073-23096.

Carlton, A. G., Bhave, P. V., Napelenok, S. L., Edney, E. O., Sarwar, G., Pinder, R. W., Pouliot, and G. A., Houyoux, M., 2010. Model representation of secondary organic aerosol in CMAQv4.7, Environmental Science and Technology, 44, 8553-8560.

Eder, B., Kang, D., Mathur, R., Pleim, J., Yu, S., Otte, T., and Pouliot, G., 2009. A performance evaluation of the National Air Quality Forecast Capability for the summer 2007, Atmospheric Environment, 43 (14), 2312-2320.

Eder, B., Yu, S., 2006. A performance evaluation of the 2004 release of Models-3 CMAQ. Atmospheric Environment 40, 4811–4824.

Foley, K. M., Roselle, S. J., Appel, K. W., Bhave, P. V., Pleim, J. E., Otte, T. L., Mathur, R., Sarwar, G., Young, J. O., Gilliam, R. C., Nolte, C. G., Kelly, J. T., Gilliland, A. B., and Bash, J. O., 2010. Incremental testing of the Community Multiscale Air Quality (CMAQ) modeling system version 4.7, Geoscientific Model Development 3, 205-226.

Grell, G. A., Dudhia, A. J., and Stauffer, D. R., 1994. A description of the Fifth-Generation PennState/NCAR Mesoscale Model (MM5). NCAR Technical Note NCAR/TN-398+STR. Available at http://www.mmm.ucar.edu/mm5/doc1.html.

Guenther, A. and Wiedinmyer, C., 2007. User's guide to the Model of Emissions of Gases and Aerosols from Nature (MEGAN), Version 2.01.

Houyoux, M. R., Vukovich, J. M., Coats Jr., C. J., Wheeler, N. J. M., Kasibhatla, P., 2000. Emission inventory development and processing for the seasonal model for regional air quality, Journal of Geophysical Research, 105 (D7), 9079 – 9090.

Otte, T. L., Pouliot, G., Pleim, J. E., Young, J. O., Schere, K. L., Wong, D. C., Lee, P. C. S., Tsidulko, M., McQueen, J. T., Davidson, P., Mathur, R., Chuang, H. Y., DiMego, G., and Seaman, N. L., 2005. Linking the Eta model with the Community Multiscale Air Quality (CMAQ) modeling system to build a national air quality forecasting system, Weather and Forecasting, 20, 367–384.

Pleim, J. E, 2007a. A combined local and nonlocal closure model for the atmospheric boundary layer. Part I: model description and testing, Journal of Applied Meteorology and Climate, 46, 1383-1395.

Pleim, J. E., 2007b. A combined local and nonlocal closure model for the atmospheric boundary layer. Part II: application and evaluation in a mesoscale meteorological model, Journal of Applied Meteorology and Climate, 46, 1396–1409.

Pouliot, G., Pierce, T., van der Gon, H. D., Schapp, M., Moran, M., and Nopmongcol, U., 2011. Comparing emission inventories and model-ready emission datasets between Europe and North America for the AQMEII project, Atmospheric Environment.

Sakulyanontvittaya, T., Duhl, T., Wiedinmyer, C., Helmig, D., Matsunaga, S., Potosnak, M., Milford, J., and Guenther, A., 2008. Monoterpene an sesquiterpene emission estimates for the United States, Environmental Science and Technology, 42, 1623-1629.

Schere, K., Flemming, J., Vautard, R., Chemel, C., Colette, A., Hogrefe, C., Bessagnet, B., Meleux, F., Mathur, R., Roselle, S., Hu, R., Sokhi, R. S., Rao, S.T., Galmarini, S., this issue. Trace gas/aerosol boundary concentrations and their impacts on continental-scale AQMEII modeling domains, Atmospheric Environment (this issue).

Skamarock, W. C., Klemp, J. B., Dudhia, J., Gill, D. O., Barker, D. M., Duda, M. G., Huang, X-Y, Wang, W., and Powers, J. G., 2008. A description of the advanced research WRF version 3. NCAR Tech Note NCAR/TN 475 STR, 125 pp, [Available from UCAR Communications, P.O. Box 3000, Boulder, CO 80307.].

Sofiev, M., Vankevich, R., Lotjonen, M., Prank, M., Petukhov, V., Ermakova, T., Koskinen, J., and Kokkonen, J., 2009. An operational system for the assimilation of satellite information on wild-land fires for the needs of air quality modeling and forecasting. Atmospheric Chemistry and Physics, 9, 6833-6847.

Tesche, T. W., Morris, R., Tonnesen, G., McNally, D., Boylan, J., and Brewer, P. 2006. "CMAQ/CAMx annual 2002 performance evaluation over the eastern US." Atmospheric Environment 40 (26), 4906-4919.

Vautard, R., Moran, M. D., Solazzo, E., Gilliam, R. C., Matthias, V., Bianconi, R., Chemel, C., Ferreira, J., Geyer, B., Hansen, A. B., Jericevic, A., Prank, M., Segers, A., Silver, J. D., Werhahn, J., Wolke, R., Rao, S. T., and Galmarini, S., (this issue). Evaluation of the meteorological forcing used for the Air Quality Model Evaluation International Initiative (AQMEII) air quality simulations, Atmospheric Environment (this issue).

Yarwood, G., Roa, S., Yocke, M., and Whitten, G., 2005. Updates to the carbon bond chemical mechanism: CB05. Final report to the US EPA, RT-0400675, available at http://www.camx.com.

Table 1. Seasonal, domain-wide MB, ME, NMB and NME for daytime (8am – 8pm LST) average O_3 for the North America (NA) AQS network and Europe (EU) AirBase network.

Season	MB (ppb)	NMB (%)	ME (ppb)	NME (%)
Winter (NA)	-3.5	-13.4	9.0	34.7
Winter (EU)	1.5	8.4	10.4	58.1
Spring (NA)	-1.8	-4.1	9.3	29.4
Spring (EU)	-1.8	-4.8	10.5	27.7
Summer (NA)	4.4	9.8	11.0	24.2
Summer (EU)	-0.7	-1.6	10.8	24.4
Fall (NA)	2.6	8.4	8.8	28.0
Fall (EU)	7.8	32.3	11.0	45.8

Table 2. Seasonal, domain-wide MB, ME, NMB and NME for daily average $PM_{2.5}$ for the North America (NA) AQS network and Europe (EU) AirBase network.

Season	MB (μgm^{-3})	NMB (%)	ME (μgm^{-3})	NME (%)
Winter (NA)	3.4	30.4	6.0	52.9
Winter (EU)	-12.9	-55.0	15.8	67.3
Spring (NA)	2.0	18.9	4.5	42.2
Spring (EU)	-5.8	-36.9	8.2	52.3
Summer (NA)	-0.6	-4.6	4.4	30.5
Summer (EU)	-4.9	-37.2	6.9	52.2
Fall (NA)	4.0	36.3	5.6	51.6
Fall (EU)	-3.8	-24.2	7.7	49.1

Table 3. Seasonal, domain-wide MB, ME, NMB and NME for daily average PM_{10} for the North America (NA) AQS and Europe (EU) AirBase network.

Season	MB (μgm^{-3})	NMB (%)	ME (μgm^{-3})	NME (%)
Winter (NA)	-11.5	-47.9	16.0	66.8
Winter (EU)	-21.5	-64.8	23.2	69.8
Spring (NA)	-14.5	-56.5	17.1	66.4
Spring (EU)	-14.0	-56.2	15.6	59.5
Summer (NA)	-16.1	-57.4	17.8	63.4
Summer (EU)	-15.1	-61.2	16.3	66.1
Fall (NA)	-11.4	-46.5	15.3	62.3
Fall (EU)	-12.2	-46.8	15.1	57.8

Figure Captions

Fig. 1. Time series of NA daytime (8am – 8pm LST) average ozone (ppb) for AQS observed (black), CMAQ using GEMS (CMAQ-GEMS) data for boundary conditions (dashed; dark grey) and CMAQ using GEOS-Chem (CMAQ-GC) data for boundary conditions (dot-dashed; light grey). The bottom plot shows the corresponding bias (ppb) for the CMAQ-GEMS simulation (solid) and CMAQ-GC simulation (dashed).

Fig. 2. Time series of EU daytime (8am – 8pm LST) average ozone (ppb) for AirBase observed (black), CMAQ using GEMS (CMAQ-GEMS) data for boundary conditions (dashed; dark grey) and CMAQ using GEOS-Chem (CMAQ-GC) data for boundary conditions (dot-dashed; light grey). The bottom plot shows the corresponding bias (ppb) for the CMAQ-GEMS simulation (solid) and CMAQ-GC simulation (dashed).

Fig. 3. Normalized mean bias (%) for daytime (8am – 8pm LST) average ozone for the North America AQS (triangles) and NAPS (circles) networks for a) winter b) spring c) summer and d) fall. Warm colors indicate positive NMBs; cool colors indicate negative NMBs; grey shading indicates NMBs less than ±10%.

Fig. 4. Normalized mean bias (%) for daytime (8am – 8pm LST) average O_3 for the Europe AirBase (circles), AURN (triangles) and EMEP (squares) networks for a) winter b) spring c) summer and d) fall. Warm colors indicate positive NMBs; cool colors indicate negative NMBs; grey shading indicates NMBs less than ±10%.

Fig. 5. Time series of daily average $PM_{2.5}$ (μgm^{-3}) for AQS observed (solid) and CMAQ estimated (dashed) for the entire U.S. The bottom time series plot shows the corresponding bias (μgm^{-3}).

Fig. 6. Time series of daily average $PM_{2.5}$ (μgm^{-3}) for AirBase observed (solid) and CMAQ estimated (dashed) for Europe. The bottom time series plot shows the corresponding bias ($\mu g\ m^{-3}$).

Fig. 7. Normalized mean bias (%) for $PM_{2.5}$ for the North America IMPROVE (circles), CSN (triangles), NAPS (squares) and AQS (diamonds) networks for a) winter b) spring c) summer and d) fall. Warm colors indicate positive NMBs; cool colors indicate negative NMBs; grey shading indicates NMBs less than ±10%.

Fig. 8. Normalized mean bias (%) for $PM_{2.5}$ for the Europe AirBase (circles), AURN (triangles), and EMEP (squares) networks for a) winter b) spring c) summer and d) fall. Warm colors indicate positive NMBs; cool colors indicate negative NMBs; grey shading indicates NMBs less than ±10%.

Fig. 9. Time series of daily average PM_{10} (μgm^{-3}) for AQS observed (solid) and CMAQ estimated (dashed) for North America. The bottom plot shows the corresponding bias (μgm^{-3}).

Fig. 10. Time series of daily average PM_{10} (μgm^{-3}) for AirBase observed (solid) and CMAQ estimated (dashed) for Europe. The bottom plot shows the corresponding bias (μgm^{-3}).

Fig. 11. Normalized mean bias (%) for daily average PM_{10} for the North America AQS network for a) winter b) spring c) summer and d) fall. Warm colors indicate positive NMBs; cool colors indicate negative NMBs; grey shading indicates NMBs less than ±10%.

Fig. 12. Normalized mean bias (%) for daily average PM_{10} for the Europe AirBase (circles), AURN (triangles) and EMEP (squares) networks for a) winter b) spring c) summer and d) fall. Warm colors indicate positive NMBs; cool colors indicate negative NMBs; grey shading indicates NMBs less than ±10%.

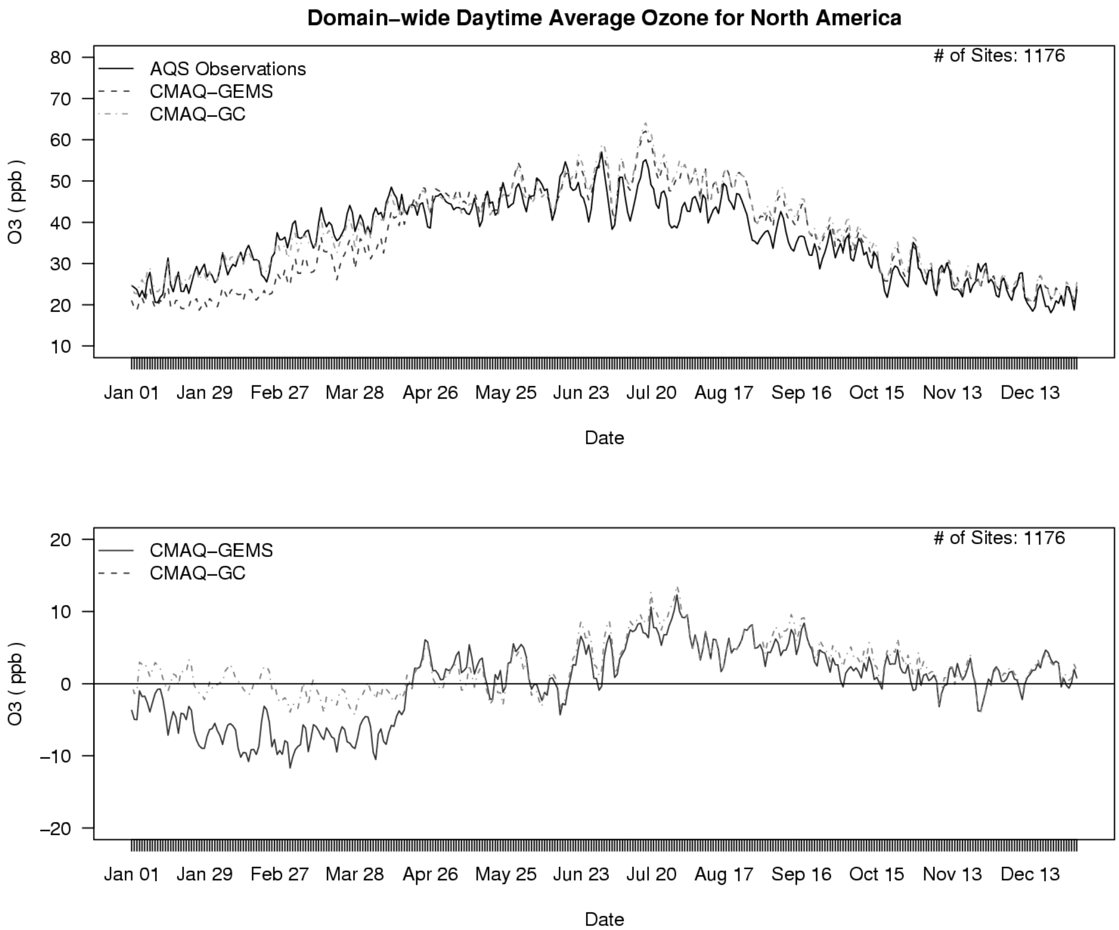

Fig. 1. Time series of NA daytime (8am – 8pm LST) average ozone (ppb) for AQS observed (black), CMAQ using GEMS (CMAQ-GEMS) data for boundary conditions (dashed; dark grey) and CMAQ using GEOS-Chem (CMAQ-GC) data for boundary conditions (dot-dashed; light grey). The bottom plot shows the corresponding bias (ppb) for the CMAQ-GEMS simulation (solid) and CMAQ-GC simulation (dashed).

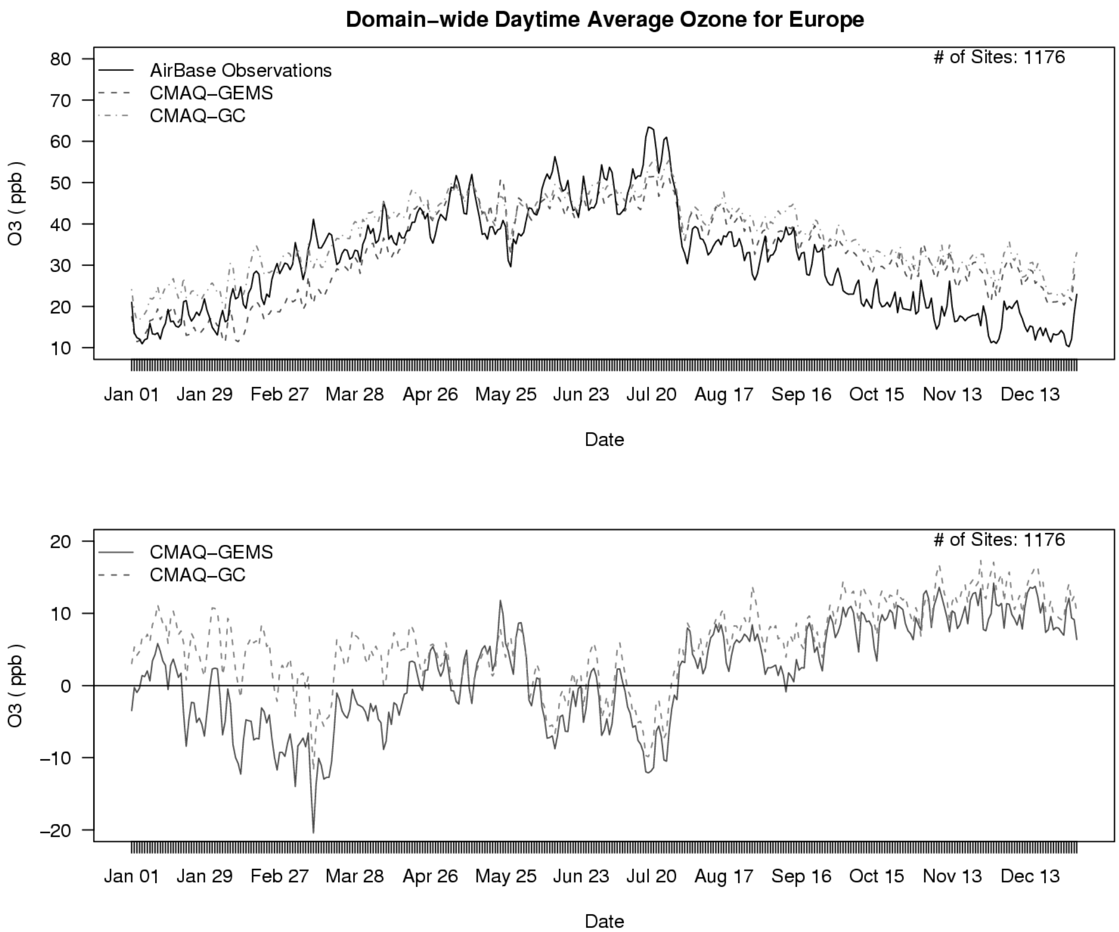

Fig. 2. Time series of EU daytime (8am – 8pm LST) average ozone (ppb) for AirBase observed (black), CMAQ using GEMS (CMAQ-GEMS) data for boundary conditions (dashed; dark grey) and CMAQ using GEOS-Chem (CMAQ-GC) data for boundary conditions (dot-dashed; light grey). The bottom plot shows the corresponding bias (ppb) for the CMAQ-GEMS simulation (solid) and CMAQ-GC simulation (dashed).

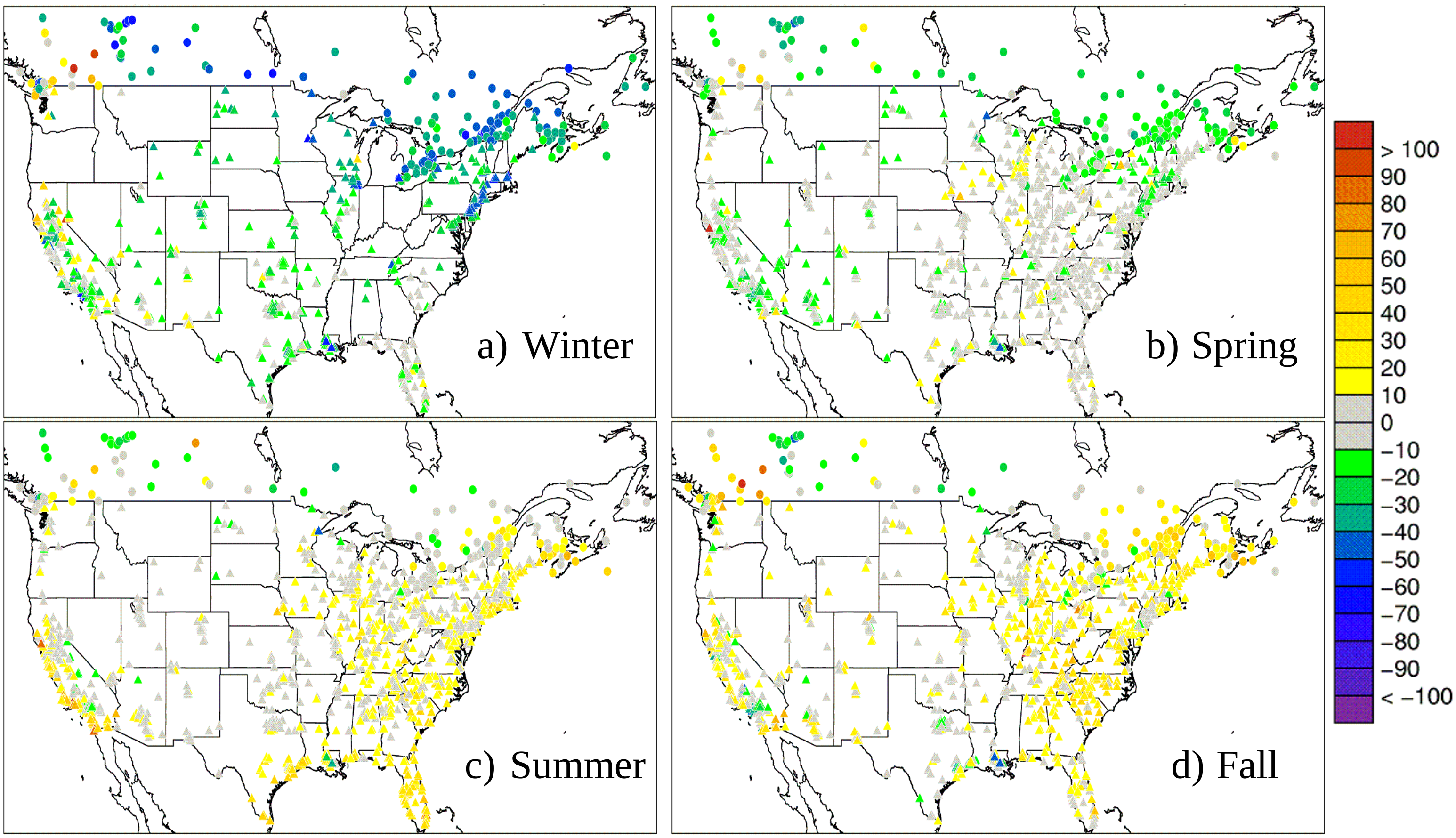

Fig. 3. Normalized mean bias (%) for daytime (8am – 8pm LST) average ozone for the North America AQS (triangles) and NAPS (circles) networks for a) winter b) spring c) summer and d) fall. Warm colors indicate positive NMBs; cool colors indicate negative NMBs; grey shading indicates NMBs less than ±10%.

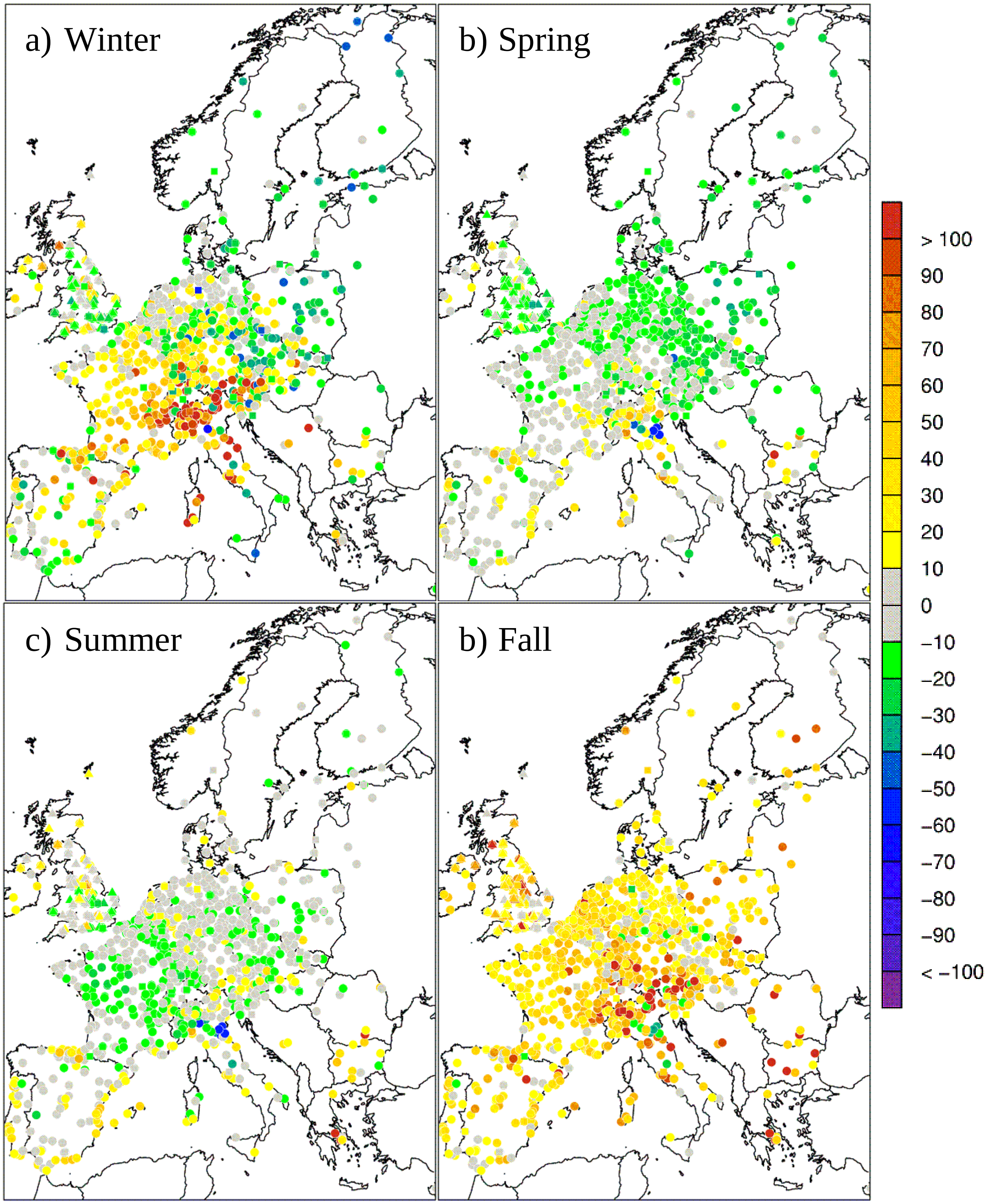

Fig. 4. Normalized mean bias (%) for daytime (8am – 8pm LST) average O_3 for the Europe AirBase (circles), AURN (triangles) and EMEP (squares) networks for a) winter b) spring c) summer and d) fall. Warm colors indicate positive NMBs; cool colors indicate negative NMBs; grey shading indicates NMBs less than ±10%.

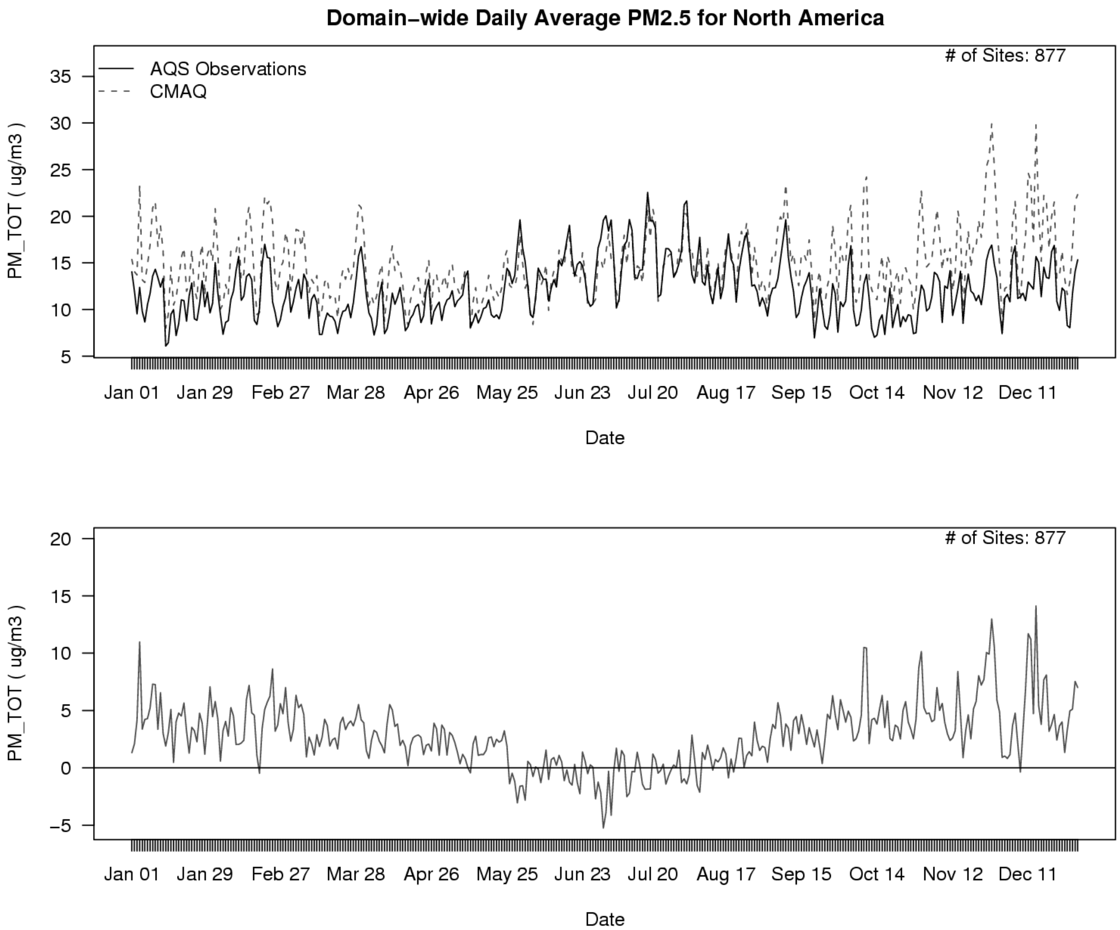

Fig. 5. Time series of daily average $PM_{2.5}$ (μgm^{-3}) for AQS observed (solid) and CMAQ estimated (dashed) for the entire U.S. The bottom time series plot shows the corresponding bias (μgm^{-3}).

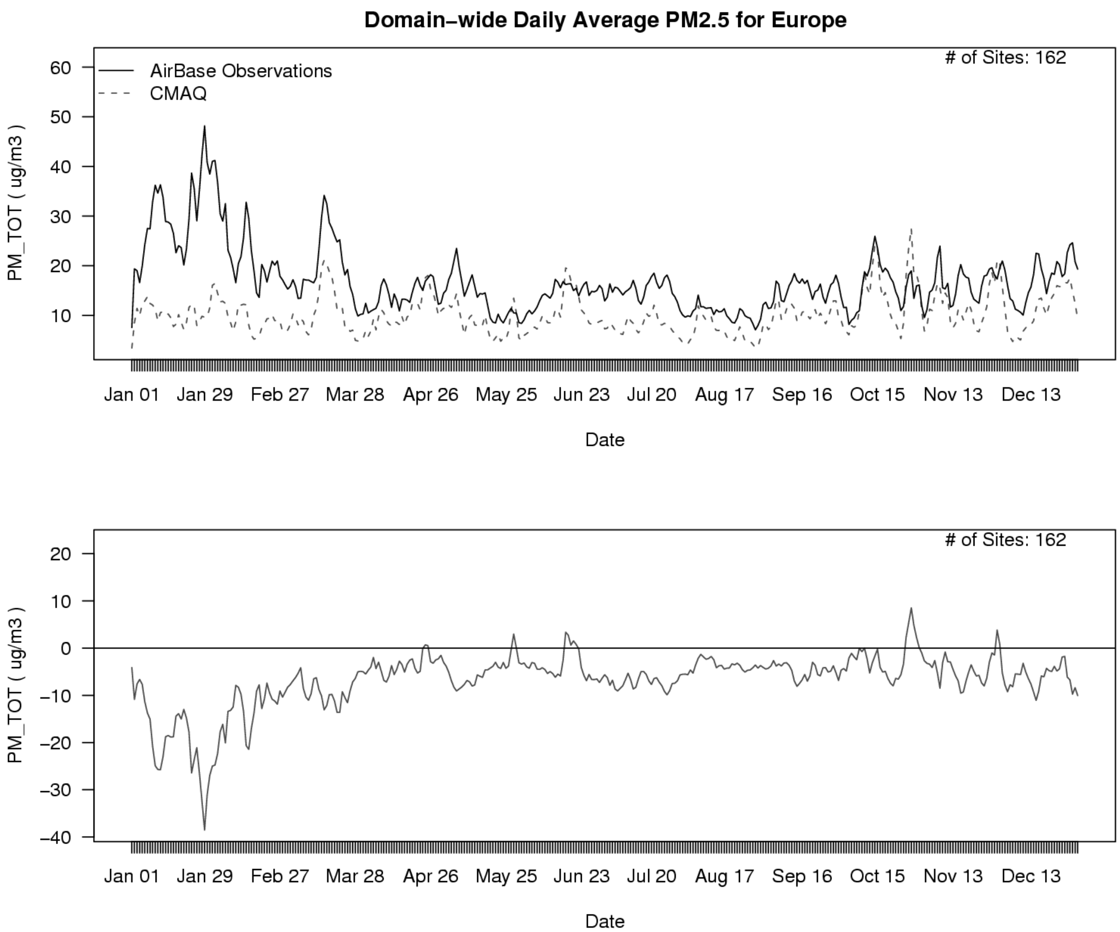

Fig. 6. Time series of daily average $PM_{2.5}$ (μgm^{-3}) for AirBase observed (solid) and CMAQ estimated (dashed) for Europe. The bottom time series plot shows the corresponding bias ($\mu g\ m^{-3}$).

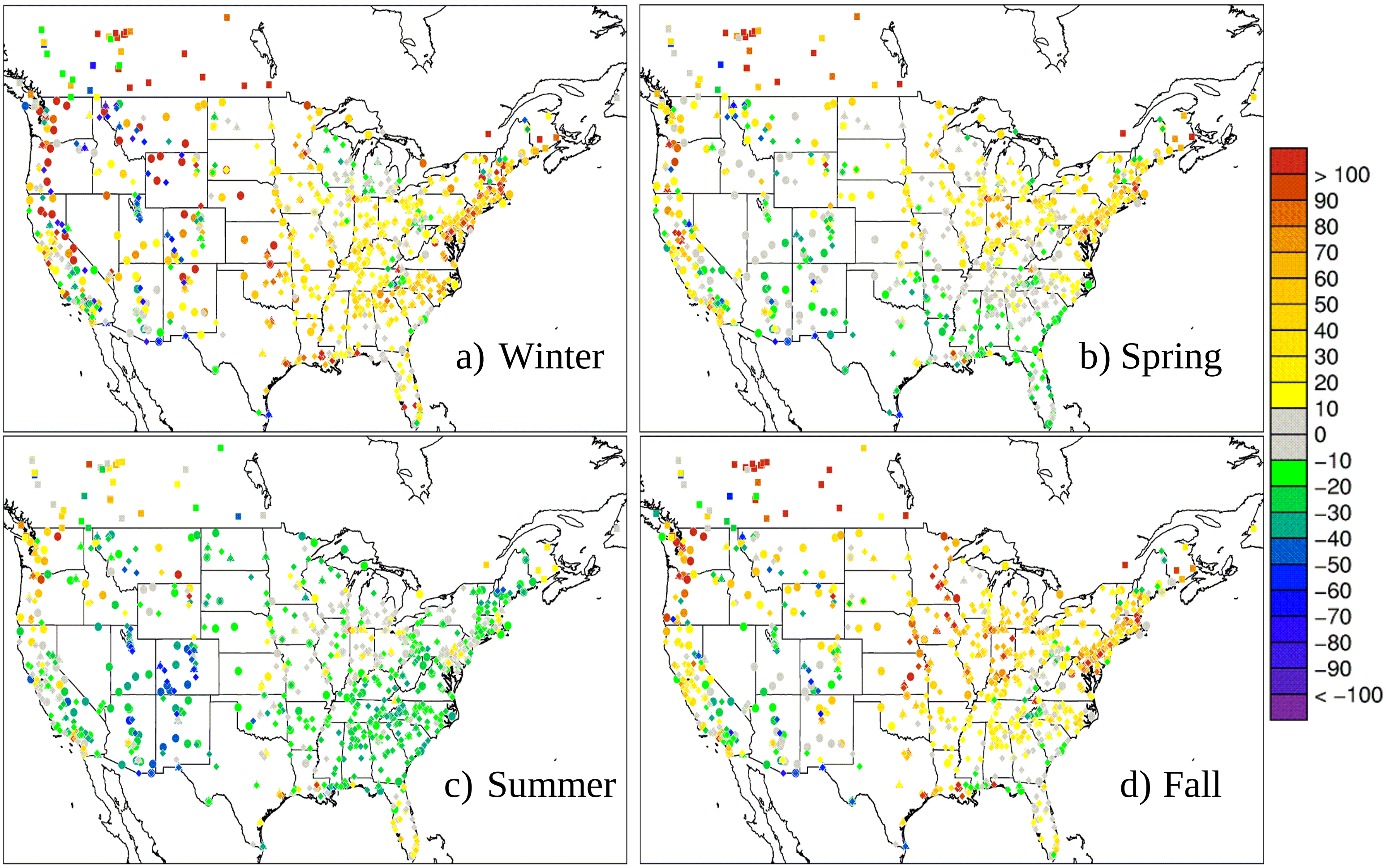

Fig. 7. Normalized mean bias (%) for $PM_{2.5}$ for the North America IMPROVE (circles), CSN (triangles), NAPS (squares) and AQS (diamonds) networks for a) winter b) spring c) summer and d) fall. Warm colors indicate positive NMBs; cool colors indicate negative NMBs; grey shading indicates NMBs less than ±10%.

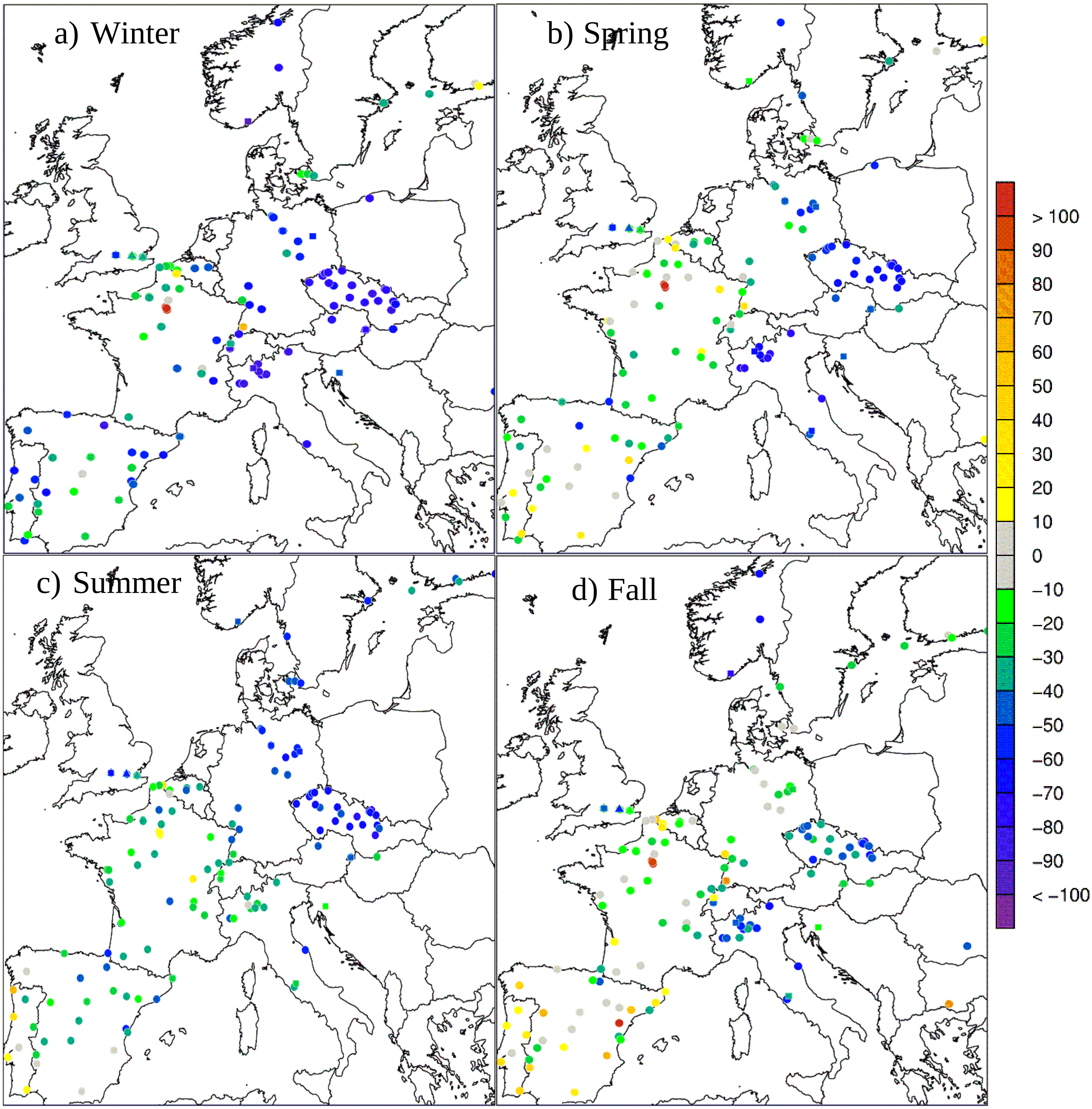

Fig. 8. Normalized mean bias (%) for $PM_{2.5}$ for the Europe AirBase (circles), AURN (triangles), and EMEP (squares) networks for a) winter b) spring c) summer and d) fall. Warm colors indicate positive NMBs; cool colors indicate negative NMBs; grey shading indicates NMBs less than ±10%.

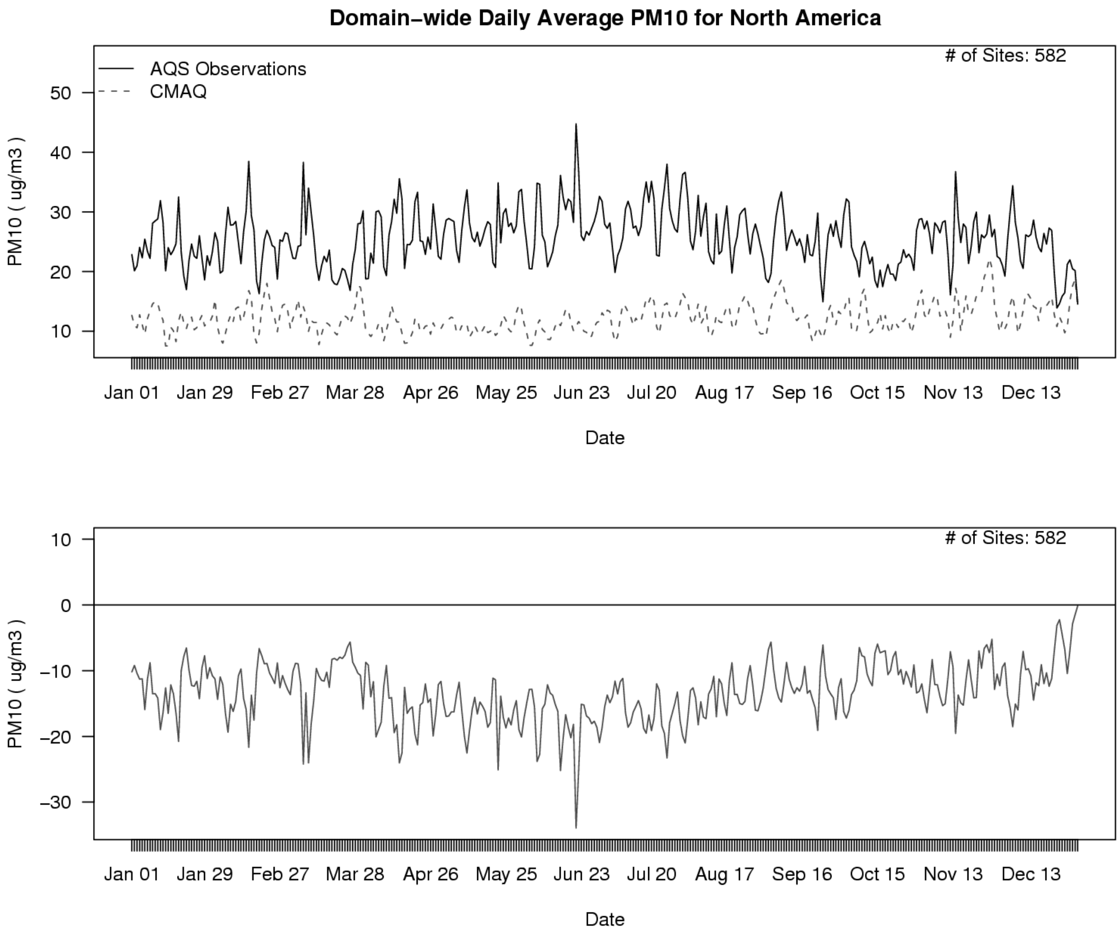

Fig. 9. Time series of daily average PM_{10} (μgm^{-3}) for AQS observed (solid) and CMAQ estimated (dashed) for North America. The bottom plot shows the corresponding bias (μgm^{-3}).

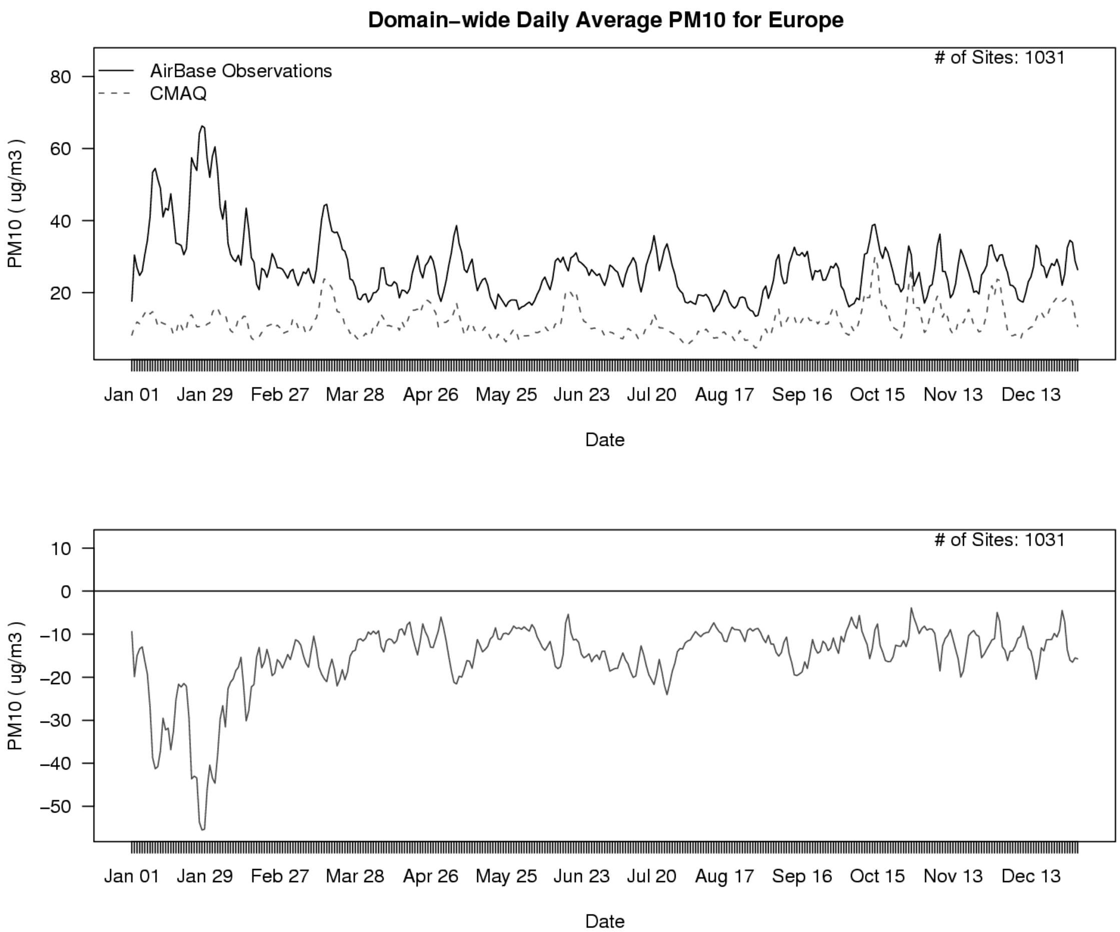

Fig. 10. Time series of daily average PM_{10} (μgm^{-3}) for AirBase observed (solid) and CMAQ estimated (dashed) for Europe. The bottom plot shows the corresponding bias (μgm^{-3}).

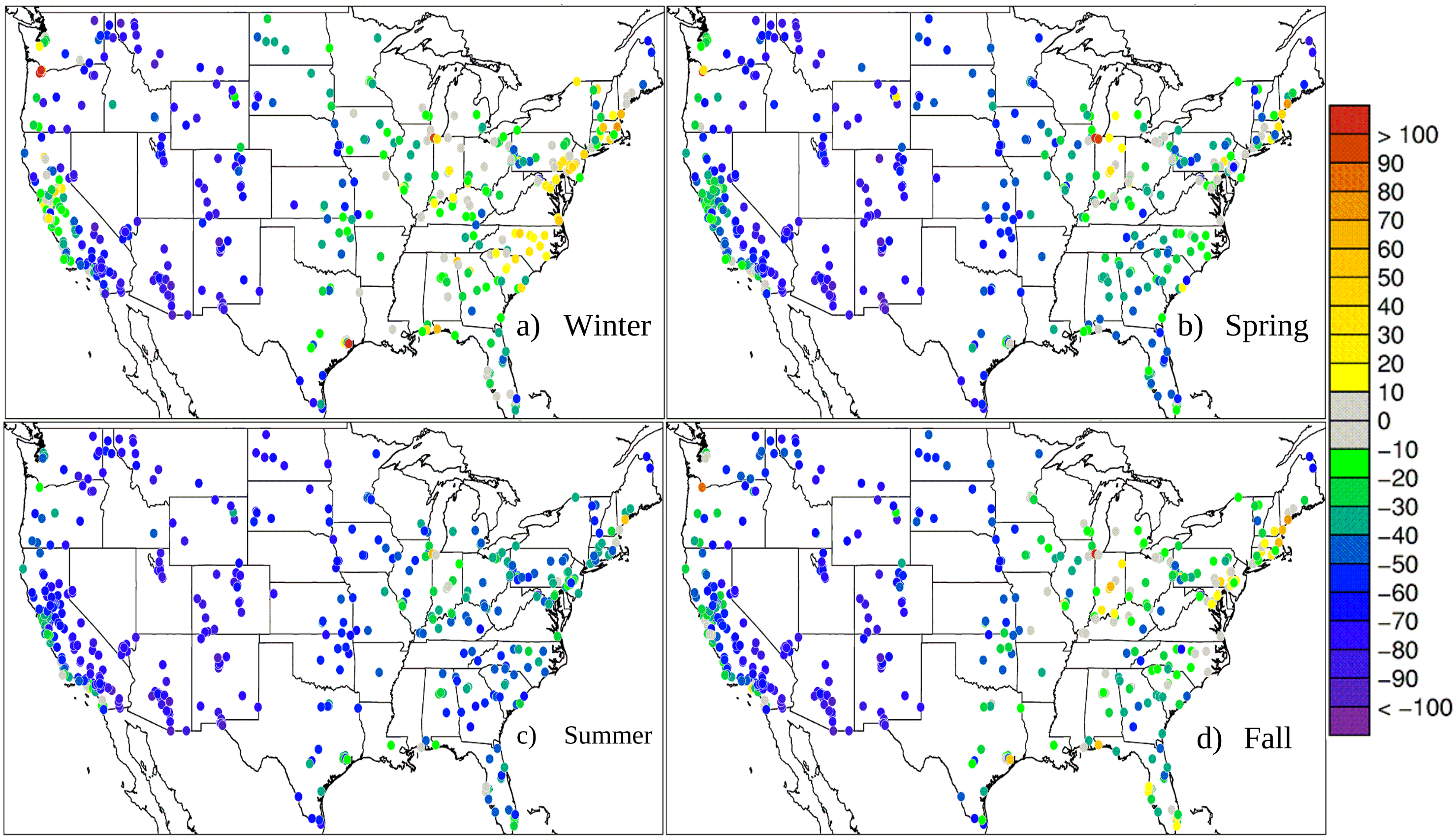

Fig. 11. Normalized mean bias (%) for daily average PM_{10} for the North America AQS network for a) winter b) spring c) summer and d) fall. Warm colors indicate positive NMBs; cool colors indicate negative NMBs; grey shading indicates NMBs less than ±10%.

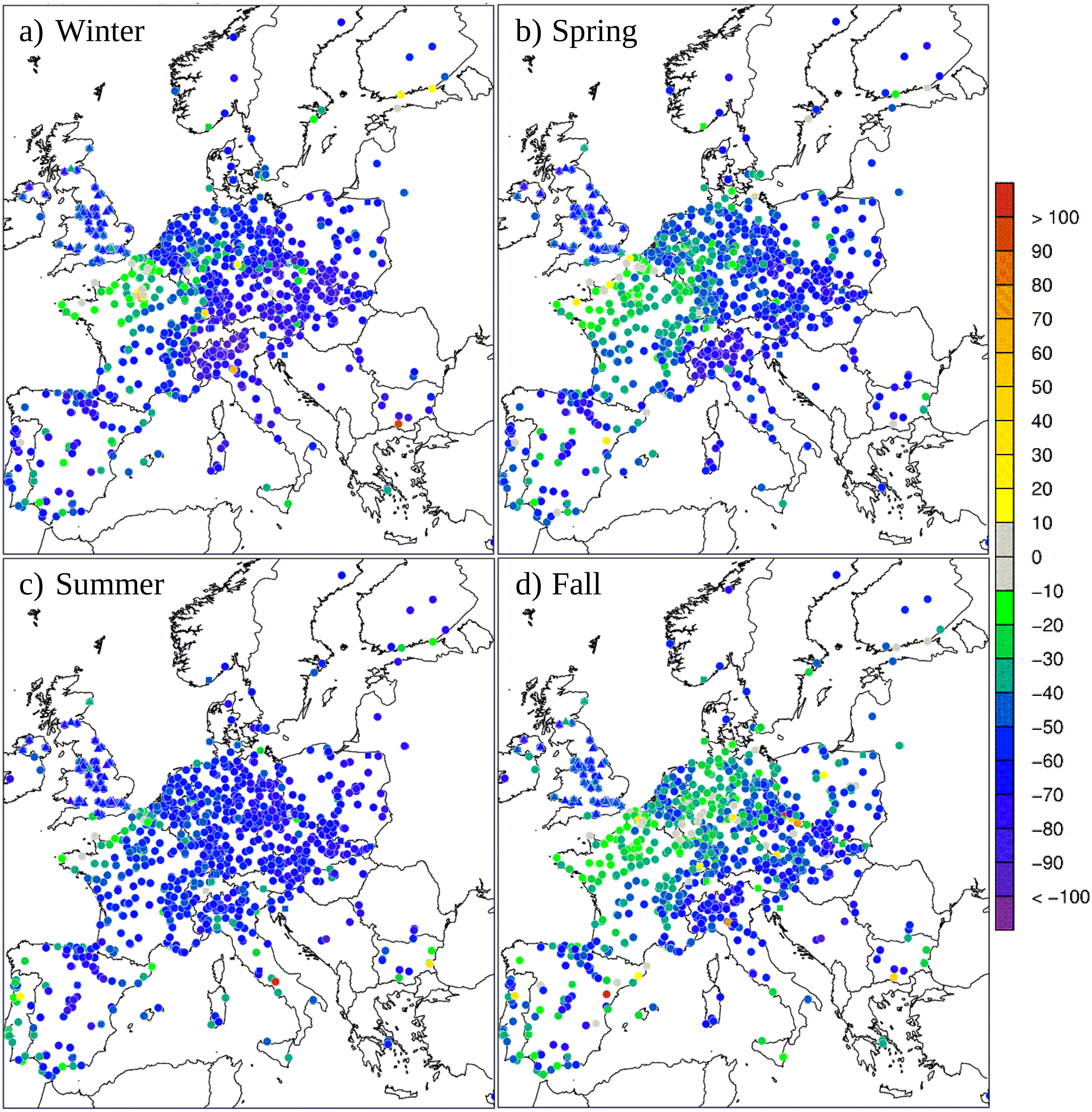

Fig. 12. Normalized mean bias (%) for daily average PM_{10} for the Europe AirBase (circles), AURN (triangles) and EMEP (squares) networks for a) winter b) spring c) summer and d) fall. Warm colors indicate positive NMBs; cool colors indicate negative NMBs; grey shading indicates NMBs less than ±10%.